Supporting Information for

Pt(II)C^N^N-Based Luminophore/Micelle Adducts for Sensing Nitroaromatic Explosives

Prasenjit Maity,*[,#] Aarti Bhatt,[#] Bhavesh Agrawal,[#] and Atanu Jana*[,†,‡]

[#]*Institute of Research and Development, Gujarat Forensic Sciences University, Gandhinagar – 382007, India*
[†]*Department of Chemistry, University of Sheffield, Sheffield, S3 7HF, UK*
[‡]*Present Address: Institute for Supramolecular Chemistry and Catalysis, Shanghai University, Shanghai, 200444, China*
E-mails: pmaity@gfsu.edu.in; atanu.j78@gmail.com

Table of Contents

A. General Experimental Section

Materials. 2-acetyl-6-bromopyridine, Phenylboronic acid, DMF-dimethylacetal, hydrazine hydrate, *p*-toluenesulfonyl chloride, K_2CO_3, $Pd(PPh_3)_4$, K_2PtCl_4, propyl bromide, dodecyl bromide, acetic acid and NaH (60% by weight dispersed in mineral oil) and nitroaromatic compounds were purchased from Aldrich Chemical Co. and were used as received. All the anhydrous solvents were acquired from Aldrich Chemical Co. and used as it is. All the reactions were carried out under an argon atmosphere unless noted otherwise. Chromatographic separations were performed by using 100–200 mesh silica gel and Al_2O_3 (Brockmann III) obtained from Merck.
Note: *TNT and RDX samples were provided by Gujarat Forensic Sciences Laboratory, (FSL-Gandhinagar), Gandhinagar, India. These are secondary explosive compounds and should be handeled only in small quantity with utmost care.*

Instrumentation. ^{1}H (400 and 500 MHz) and ^{13}C (100 and 125 MHz) NMR spectra were recorded using either Bruker DPX-400 or Bruker DPX-500 spectrometer in $CDCl_3$ at 298 K using either residual solvent signals or tetramethylsilane as internal standards. Chemical shifts were reported as δ in ppm. ESI-MS were recorded in a micromass LCT instrument. UV-vis spectra were recorded using a Varian Cary 50 spectrophotometer in various solvents. Luminescence spectra were measured on a JASCO FP700 spectrometer, at 298 K and 77 K respectively using various solvents.

B. Synthesis and Characterisation

Synthesis: The C^N^N-based chelate ligands and their Pt(II)-complexes are synthesized by following standard literature procedures.[S1] The synthetic route for both the ligands **1** and **2** along with their Pt(II)-complexes (**1•Pt** and **2•Pt** respectively) is summarised in Scheme S1. The final products were recrystallized from suitable solvent combinations ($CHCl_3$/Hexane) and used for characterization, photophysical analyses and surface chemical studies.

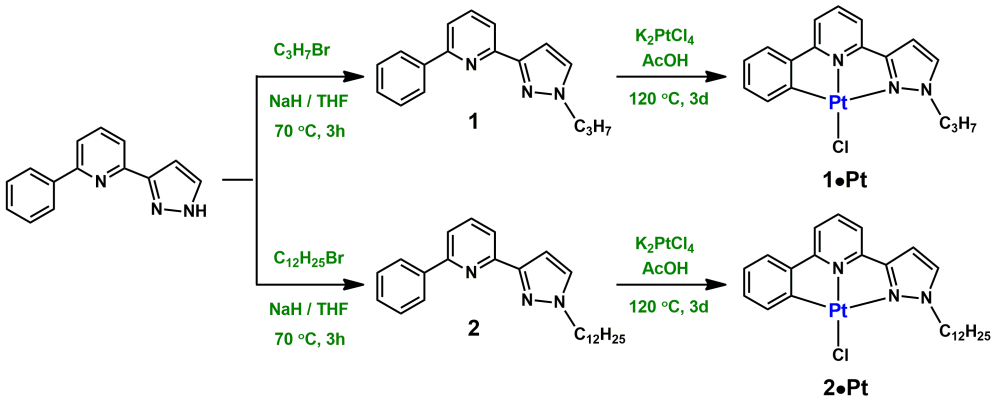

Scheme S1: Synthetic routes for ligands **1** and **2** along with their corresponding Pt(II)-complexes.

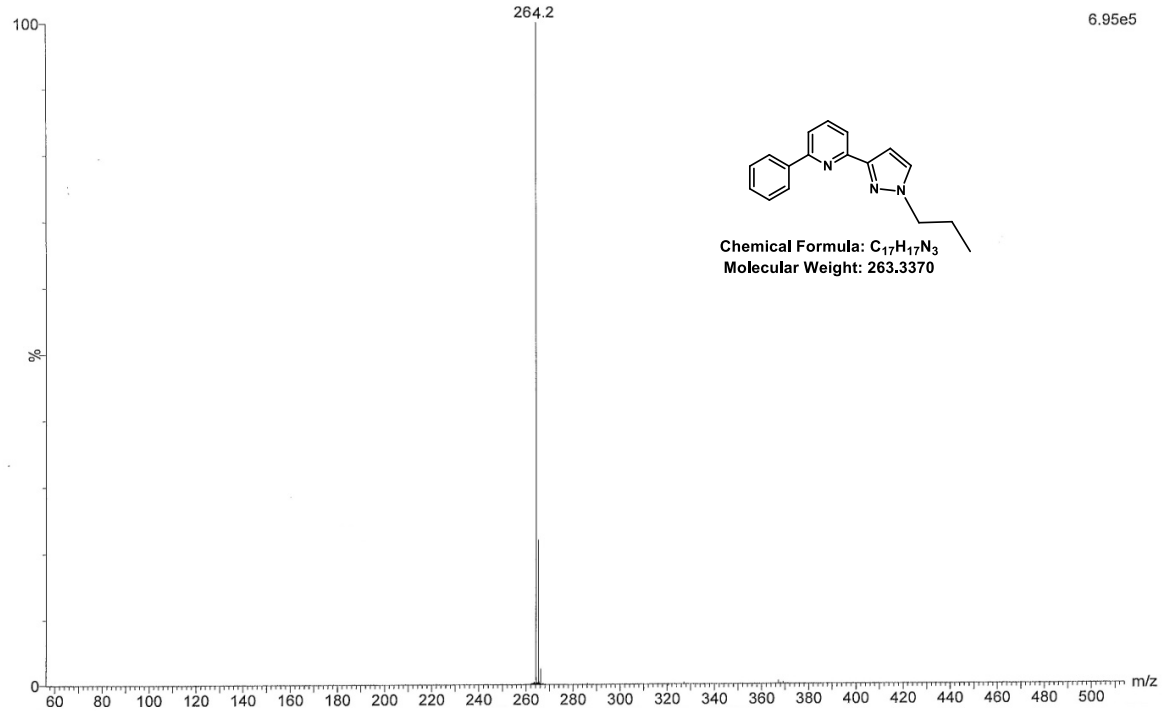

Figure S1: ESI MS of ligand **1**.

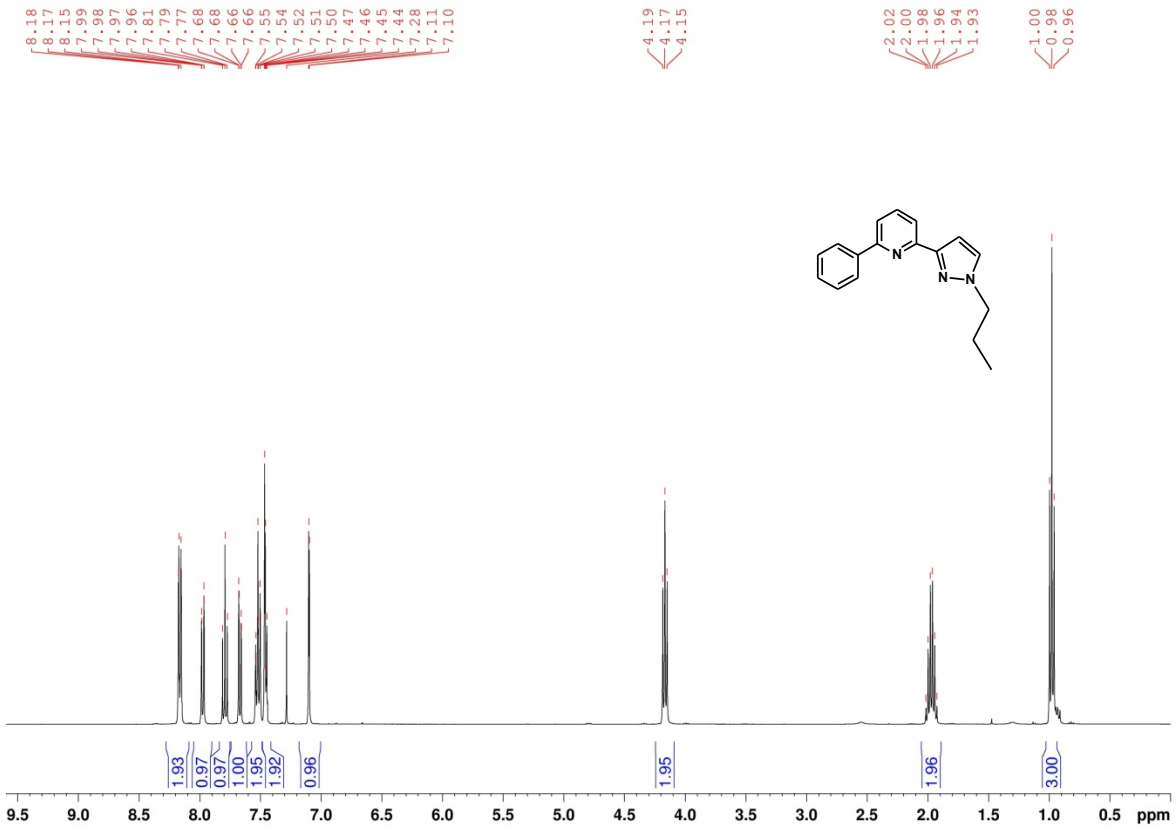

Figure S2: 400 MHz ^{1}H-NMR spectrum of ligand **1** in $CDCl_3$ at RT.

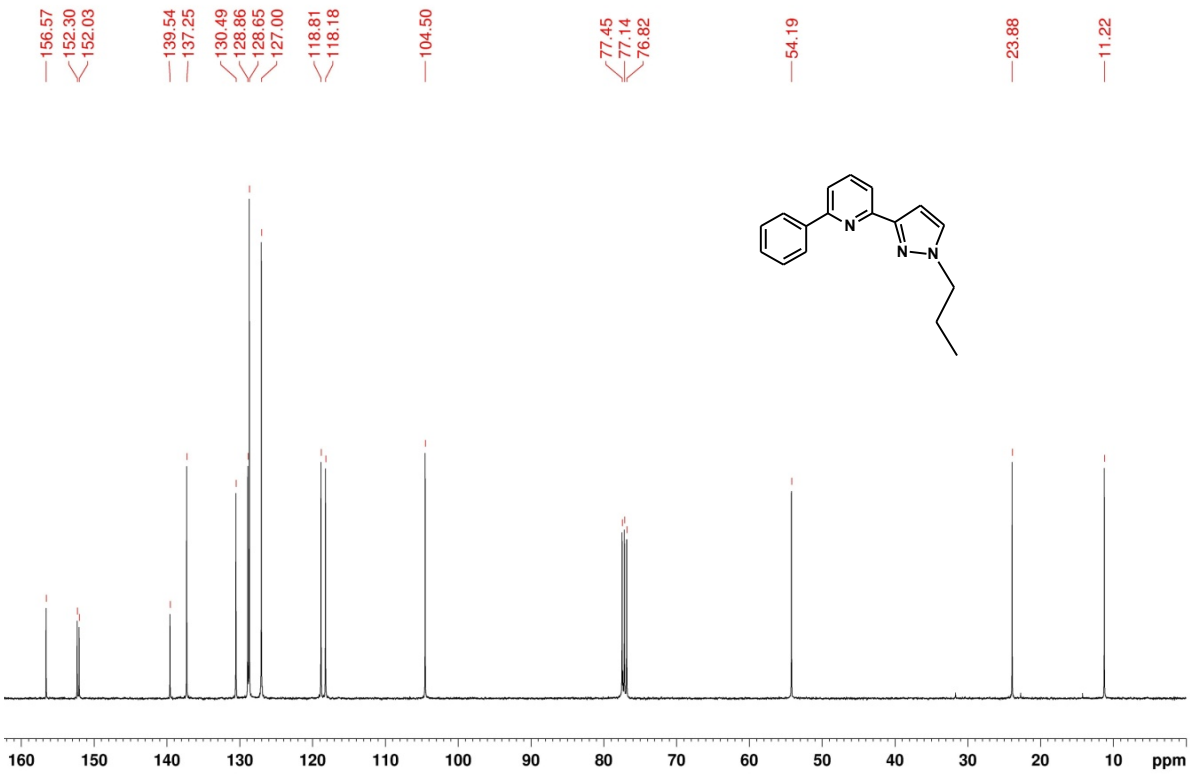

Figure S3: 100 MHz ^{13}C-NMR spectrum of ligand **1** in $CDCl_3$ at RT.

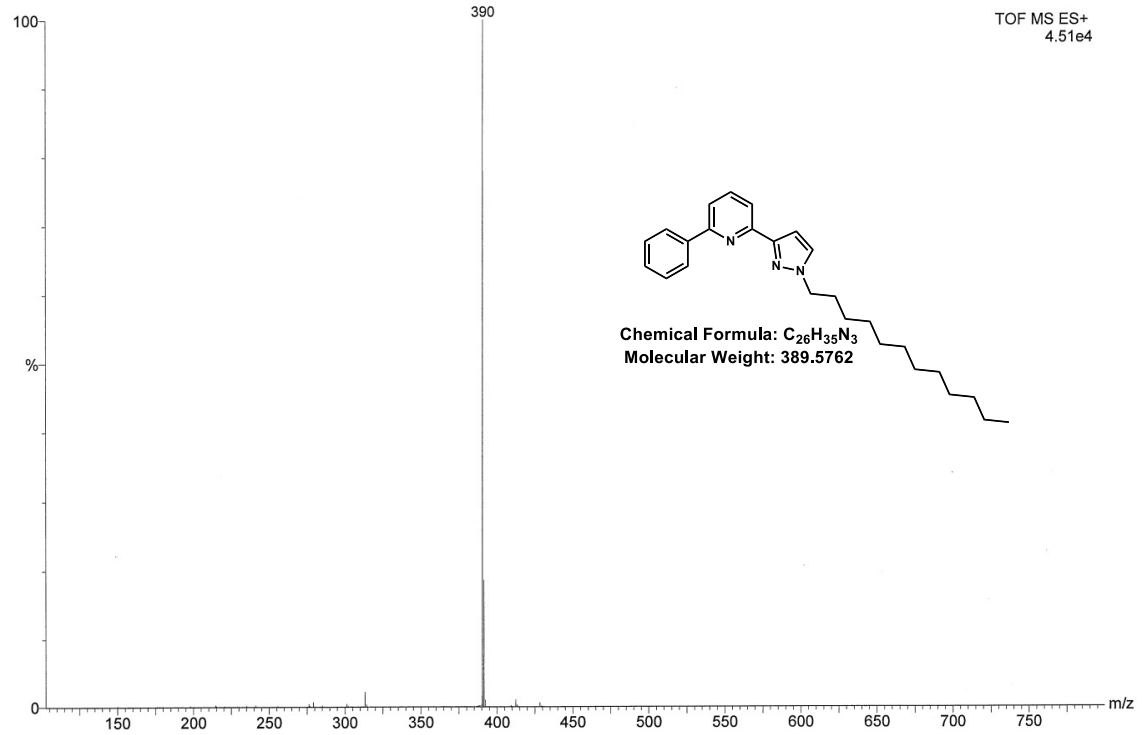

Figure S4: ESI-MS of ligand **2**.

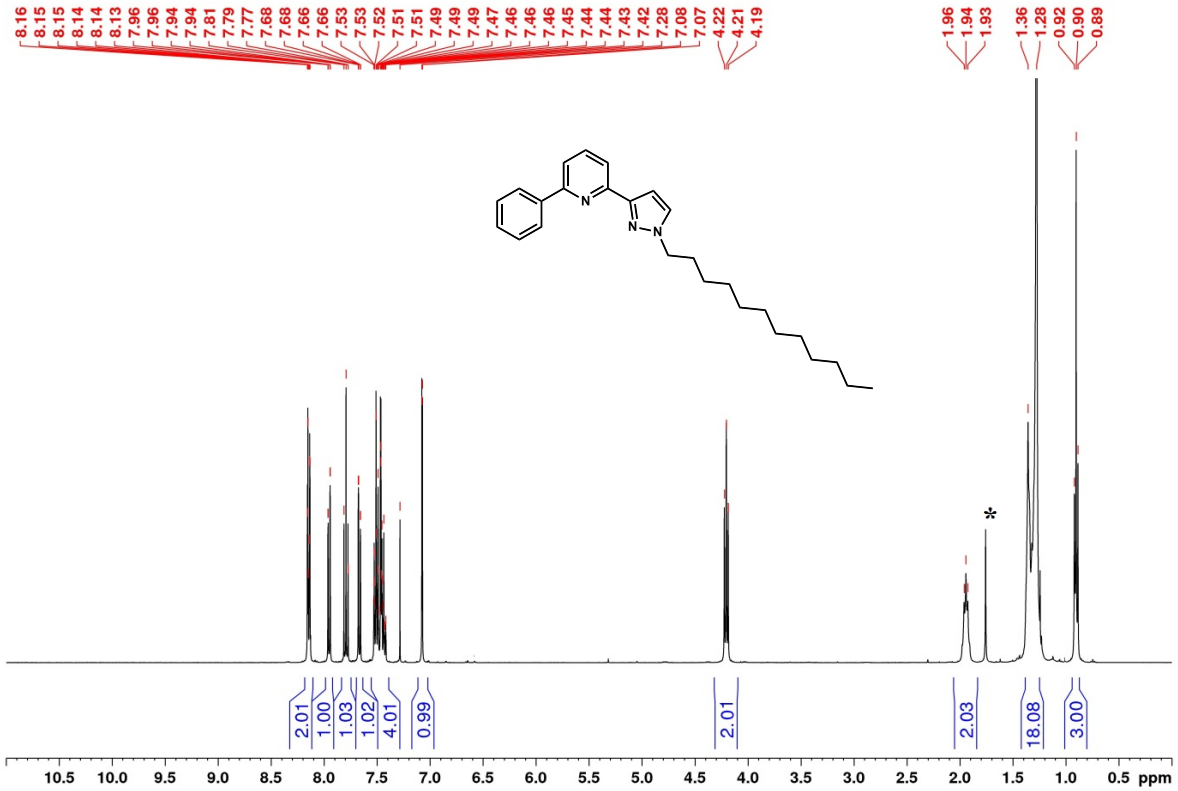

Figure S5: 400 MHz ^{1}H-NMR spectrum of ligand **2** in $CDCl_3$ at RT.

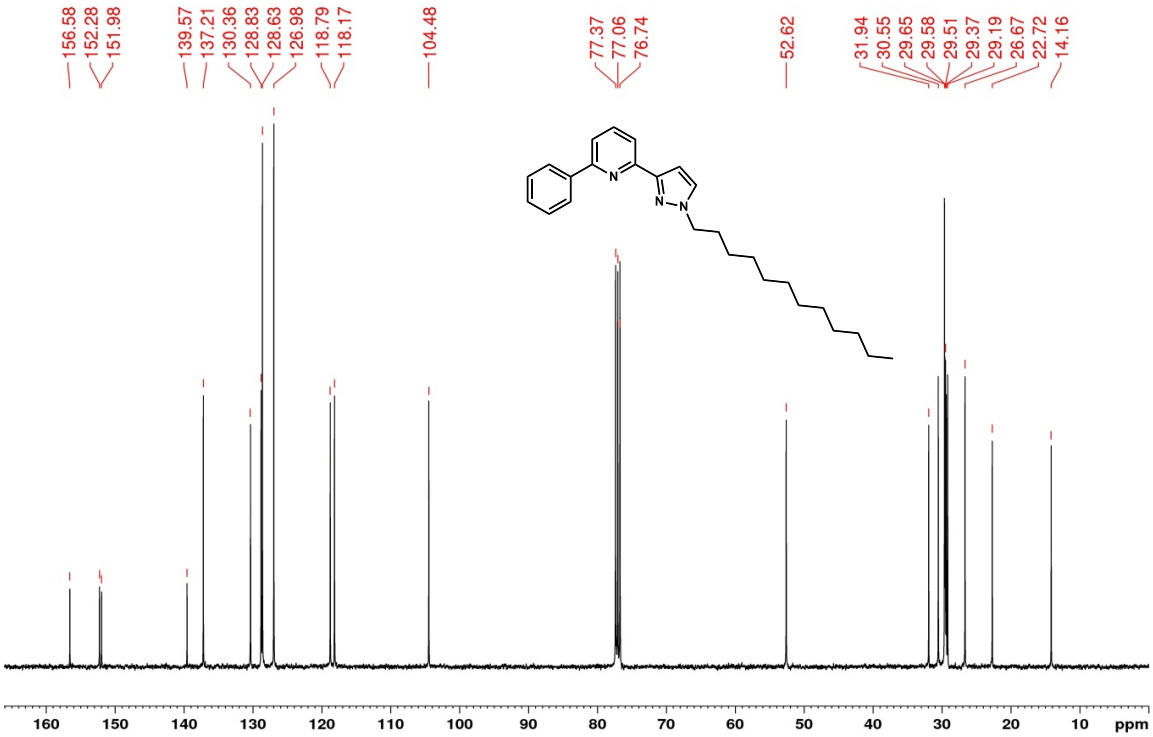

Figure S6: 100 MHz ^{13}C-NMR spectrum of ligand **2** in $CDCl_3$ at RT.

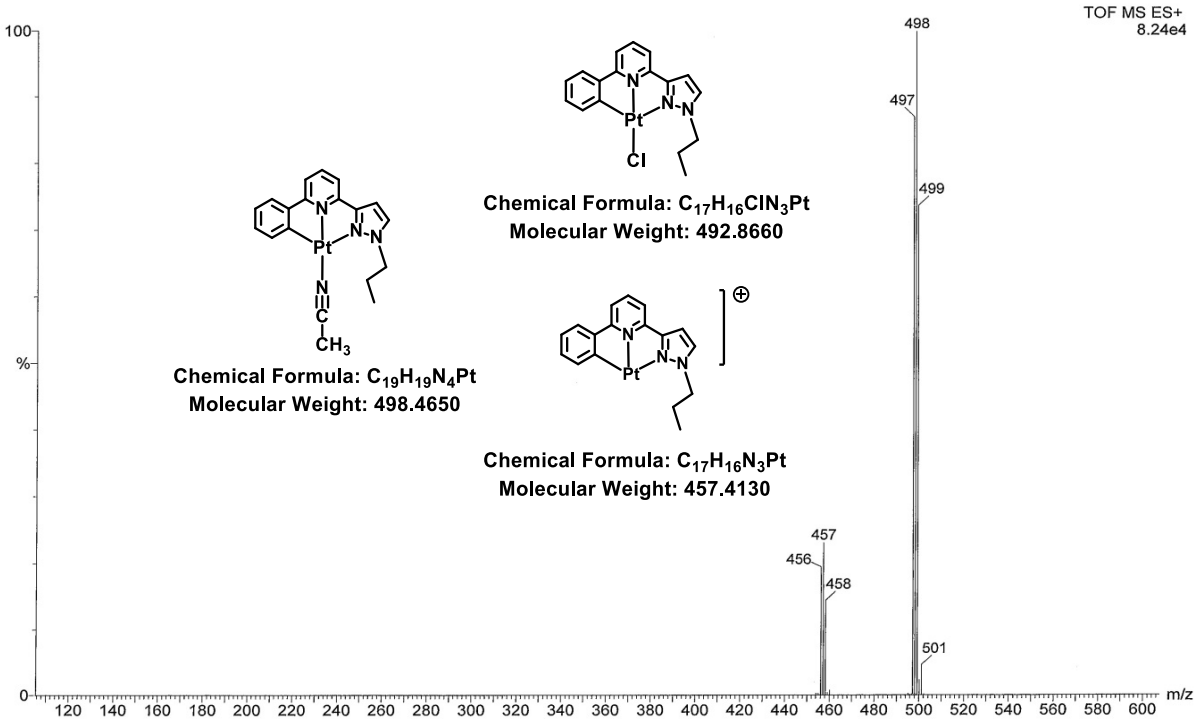

Figure S7: ESI MS of **1•Pt** complex.

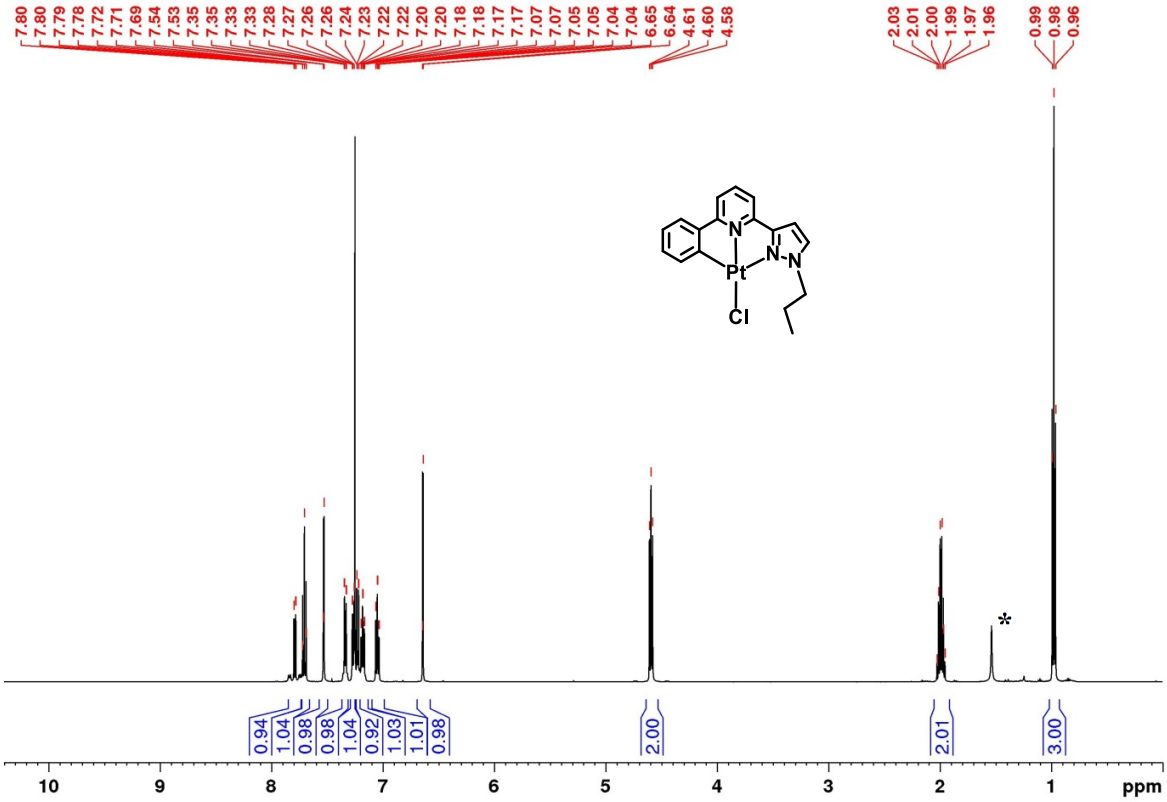

Figure S8: 500 MHz ^{1}H-NMR spectrum of **1•Pt** complex in $CDCl_3$ at RT.

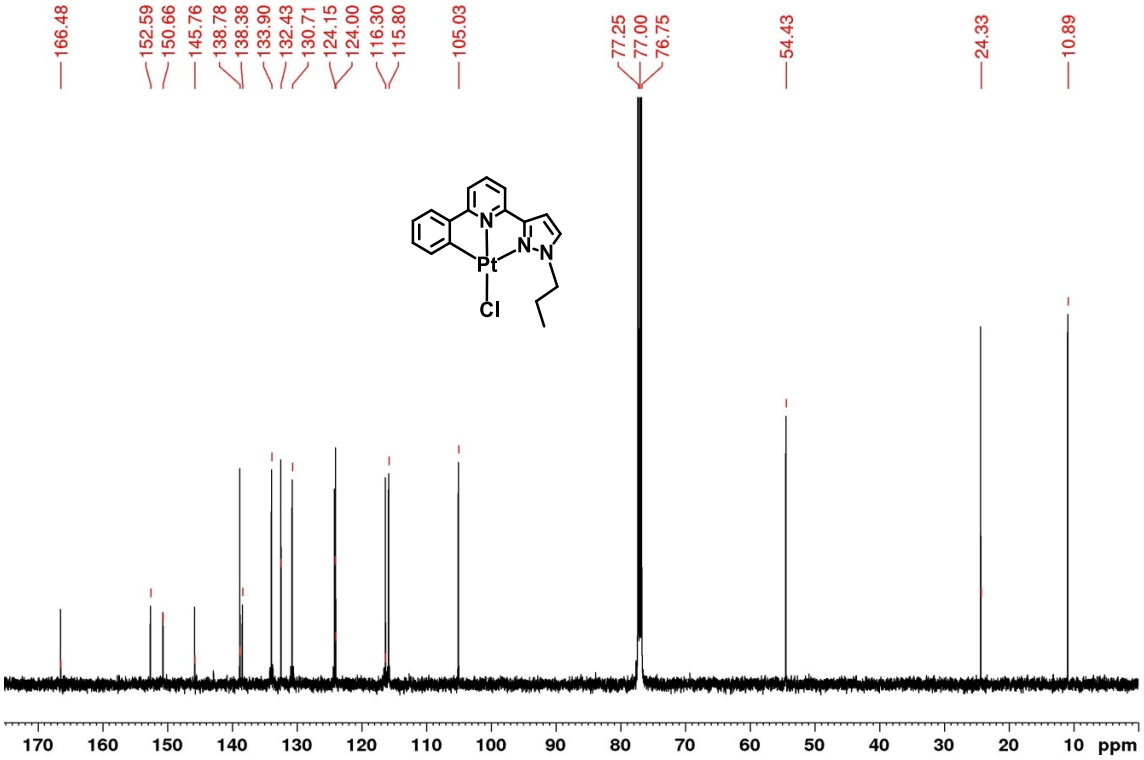

Figure S9: 125 MHz ^{13}C-NMR spectrum of **1•Pt** complex in $CDCl_3$ at RT.

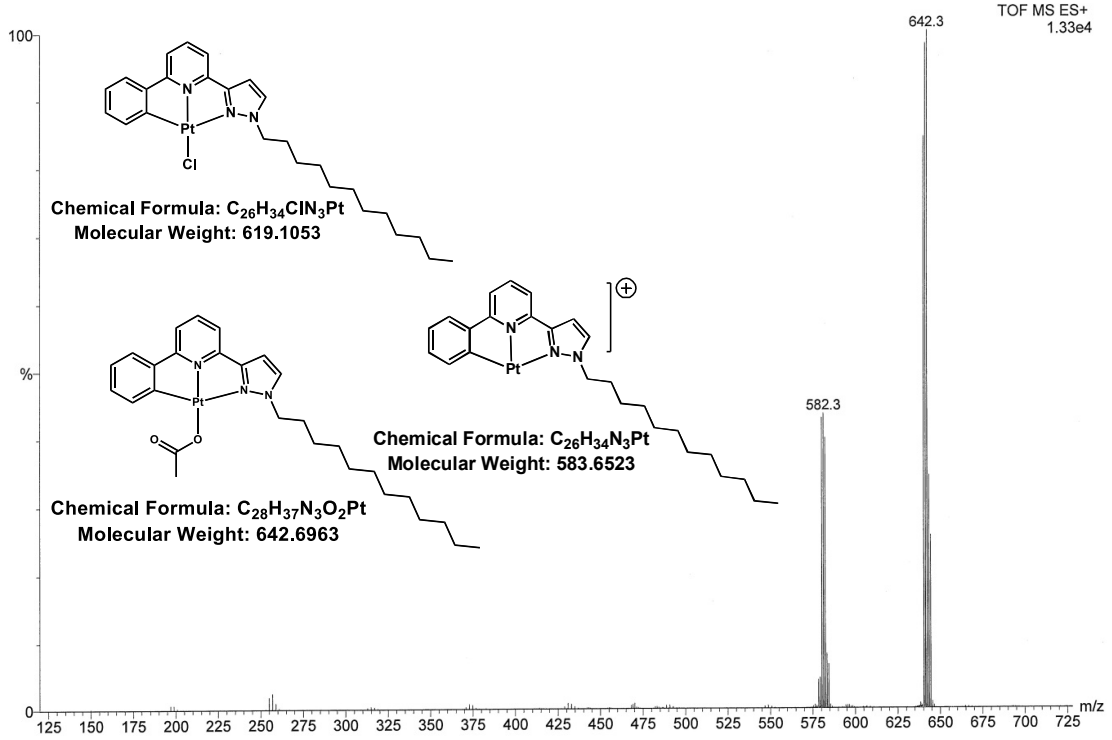

Figure S10: ESI-MS of **2•Pt** complex.

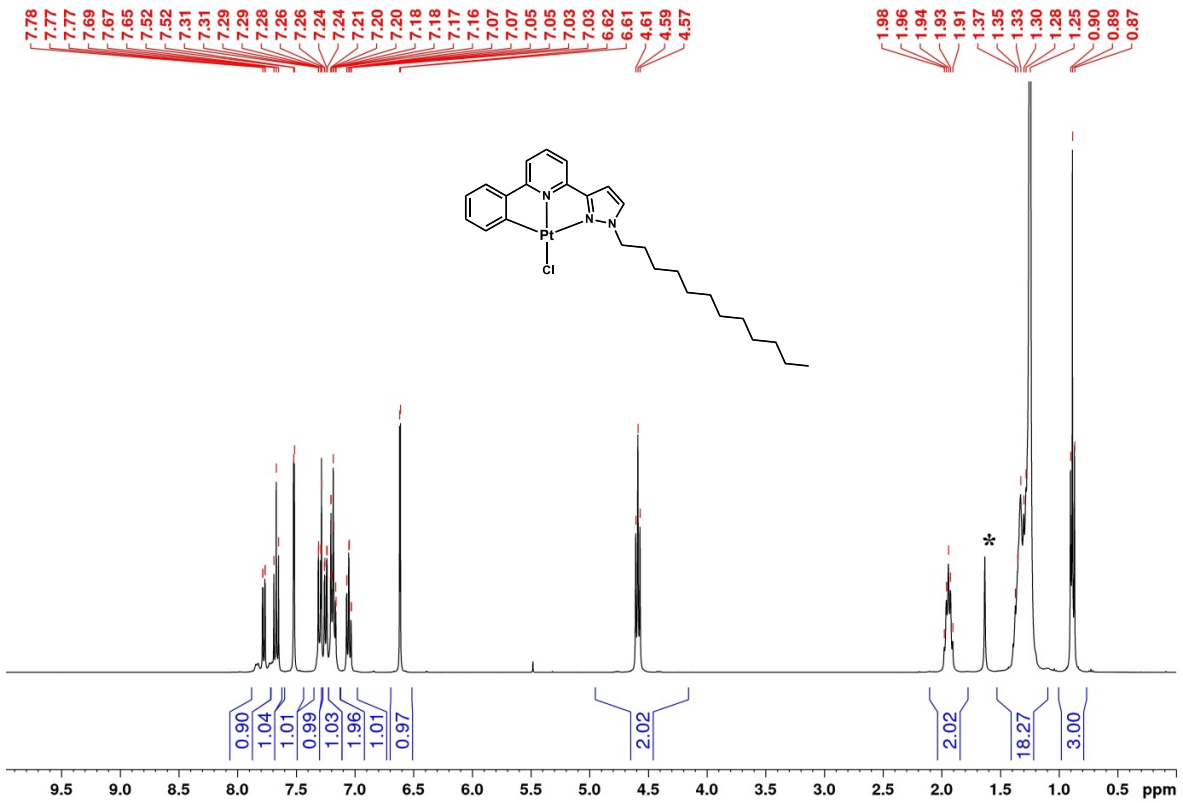

Figure S11: 400 MHz ^{1}H-NMR spectrum of **2•Pt** complex in $CDCl_3$ at RT.

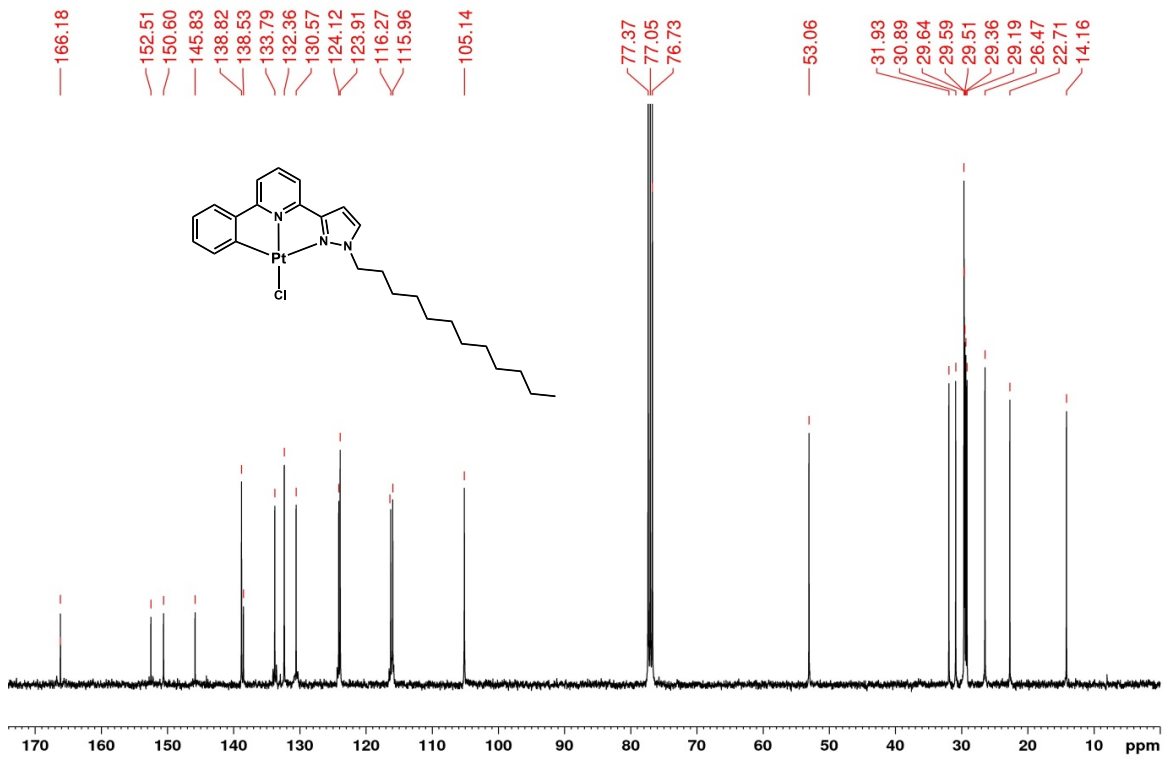

Figure S12: 100 MHz ^{13}C-NMR spectrum of **2•Pt** complex in $CDCl_3$ at RT.

C. Additional Photophysical Data

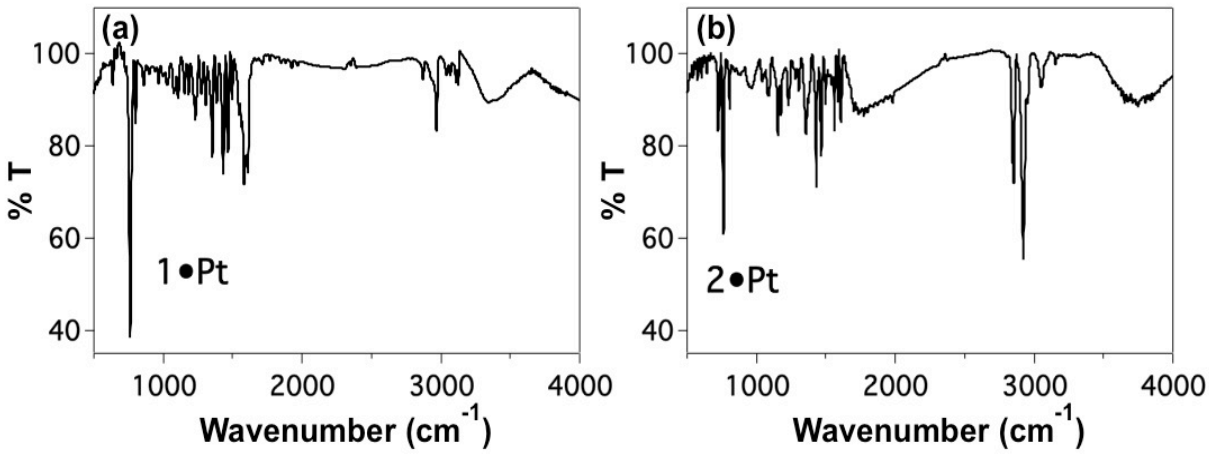

Figure S13: FTIR spectra of (a) **1•Pt** and (b) **2•Pt** measured as KBr pellet.

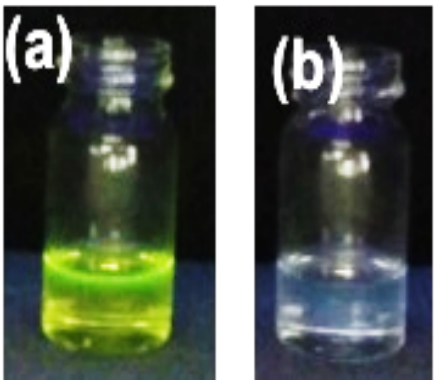

Figure S14: Visual changes of DCM solution of **2•Pt** (a) before addition and (b) after addition of TNT under 365 nm UV light.

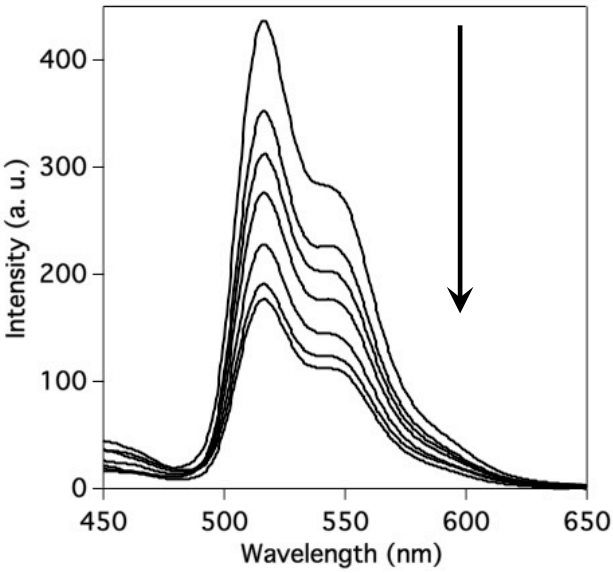

Figure S15: Emission spectra of **1•Pt** (1×10^{-5}M) in 2 mL CH_2Cl_2 with increasing amounts of TNP, the concentration of TNP from top to bottom are 0, 40, 80, 120, 160, 200 and 240 μM respectively.

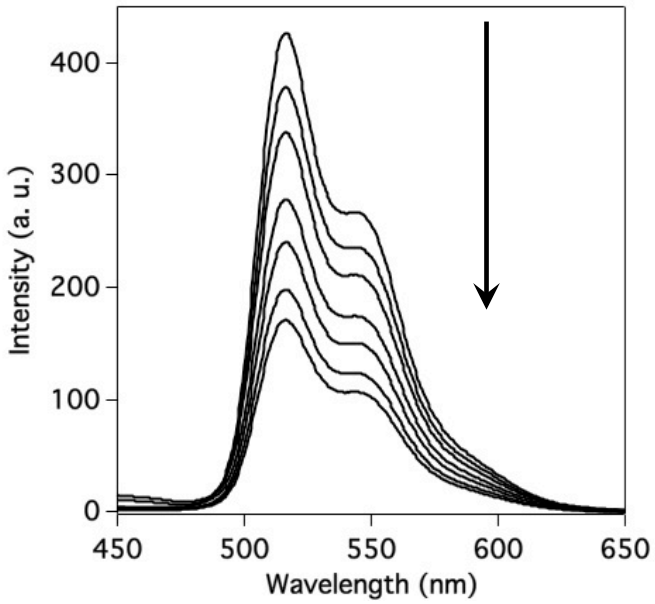

Figure S16: Emission spectra of **1•Pt** (1×10^{-5}M) in 2 mL CH_2Cl_2 with increasing amounts of TNT, the concentration of TNT from top to bottom are 0, 40, 80, 120, 160, 200 and 240 μM respectively.

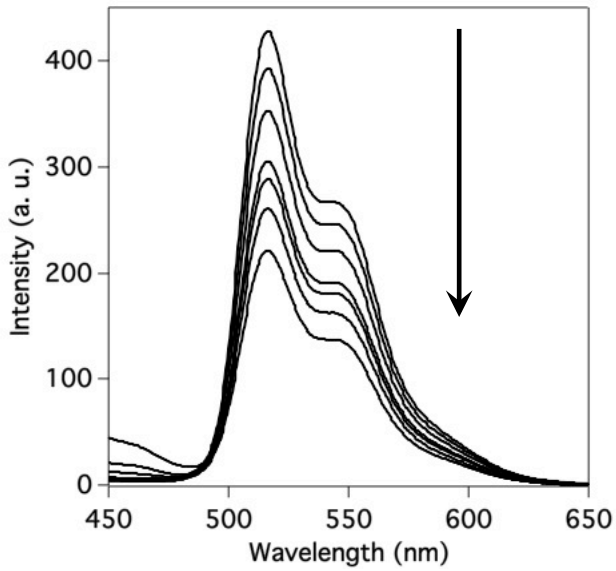

Figure S17: Emission spectra of **1•Pt** (1×10^{-5}M) in 2 mL CH_2Cl_2 with increasing amounts of DNT, the concentration of DNT from top to bottom are 0, 40, 80, 120, 160, 200 and 240 μM respectively.

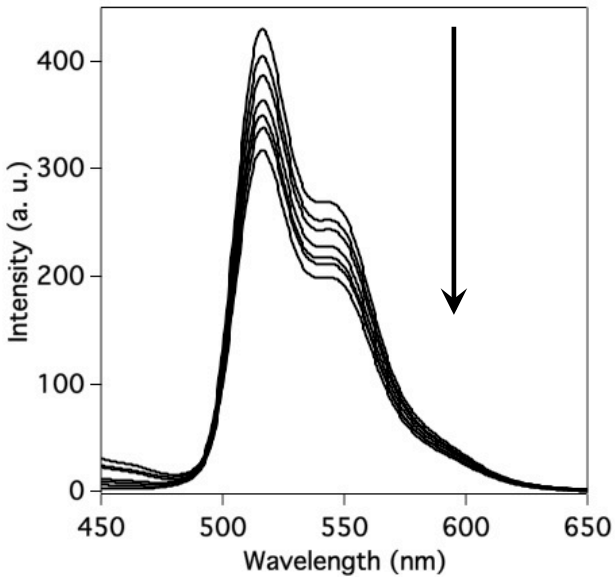

Figure S18: Emission spectra of **1•Pt** (1×10^{-5}M) in 2 mL CH_2Cl_2 with increasing amounts of NT, the concentration of NT from top to bottom are 0, 40, 80, 120, 160, 200 and 240 μM respectively.

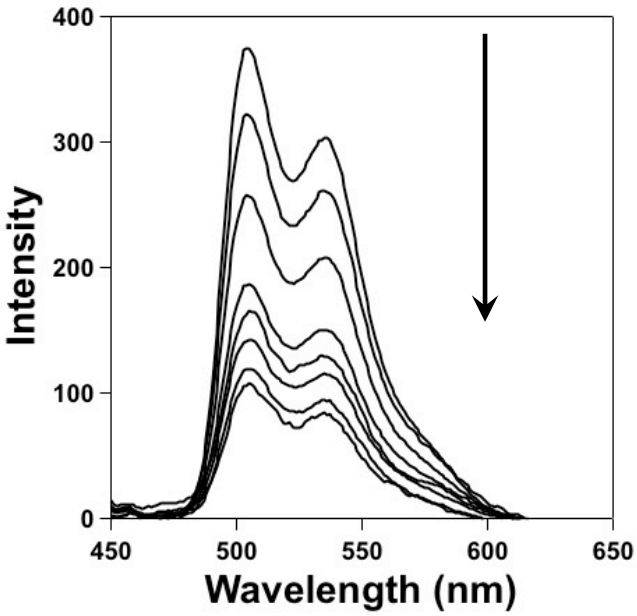

Figure S19: Emission spectra of **2•Pt** (1×10^{-5}M) in 2 mL DMSO with increasing amounts of TNP, the concentration of TNP from top to bottom are 0, 40, 80, 120, 160, 200 and 240 μM respectively.

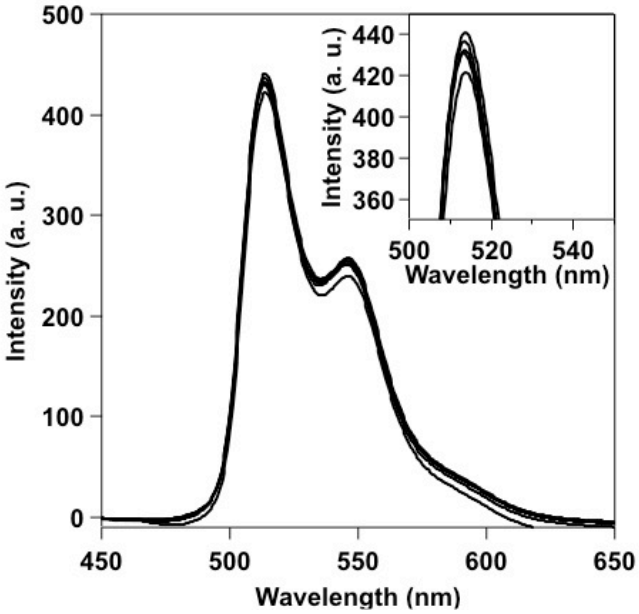

Figure S20: Emission spectra of **2•Pt** (1×10^{-5}M) in 2 mL DCM with increasing amounts of RDX, the concentration of RDX from top to bottom are 0, 40, 80, 120, 160, 200 and 240 μM respectively. Inset shows the magnified version of overlapping peaks at 514 nm.

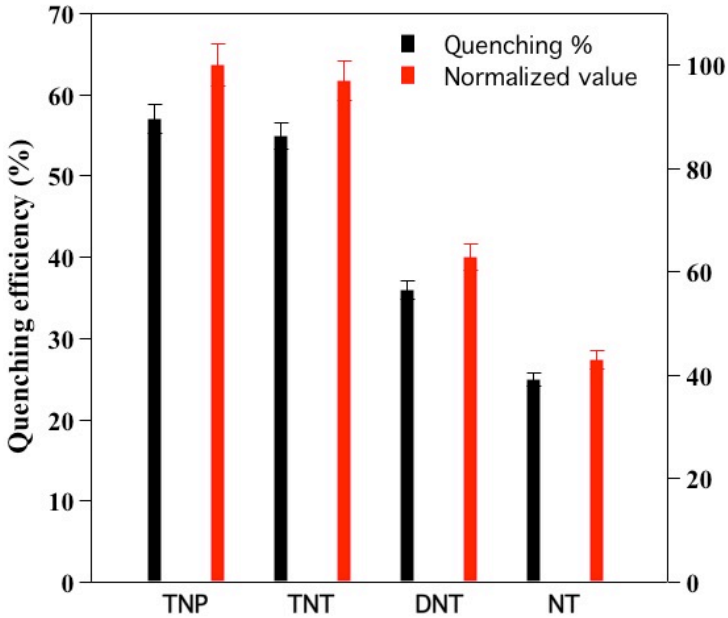

Figure S21: Fluorescence quenching efficiencies of **2•Pt** (1×10^{-5}M) in DCM after addition of 200 μM concentration of four analytes (TNP, TNT, DNT, NT). The black bars show actual quenching values (in %) and red bars represent normalized values by taking TNP quenching as 100%.

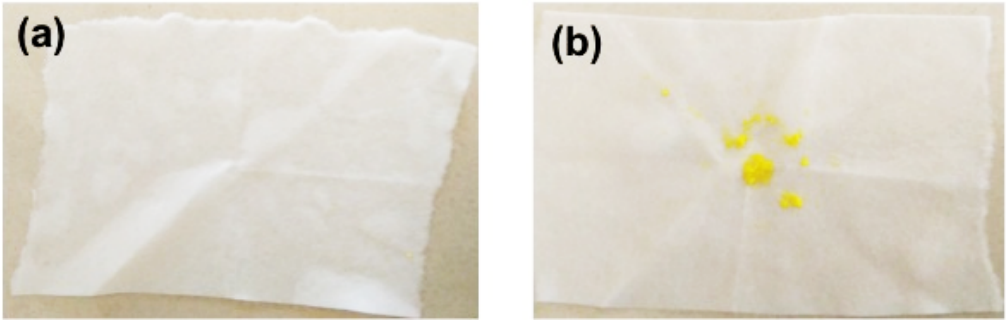

Figure S22: Photographs of filter papers used to prepare (a) **2•Pt**/Triton X-100 and (b) **1•Pt**/Triton X-100 miceller adducts, respectively, in water. The residues of **1•Pt** left on filter paper indicate that it was insignificantly soluble in miceller host due to shorter propyl chain.

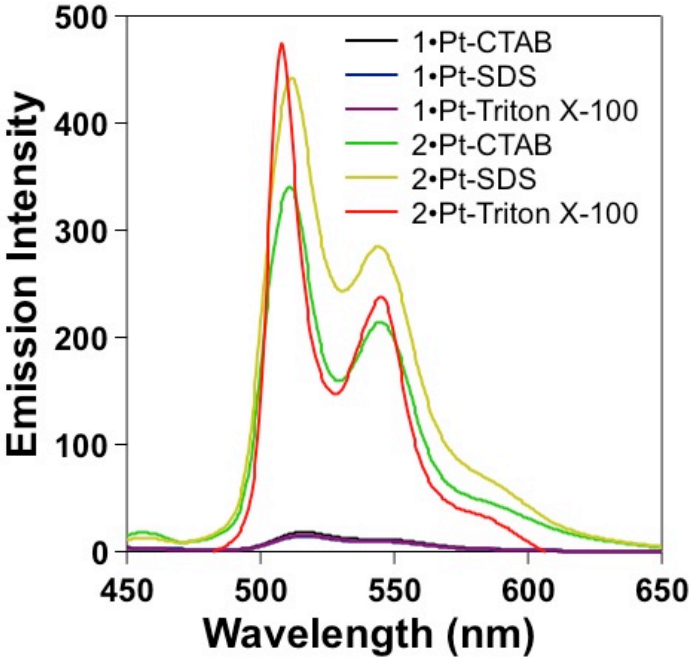

Figure S23: Emission spectra of aqueous adducts of **1•Pt** and **2•Pt** with three different surfactants, viz. Triton X-100, SDS and CTAB respectively.

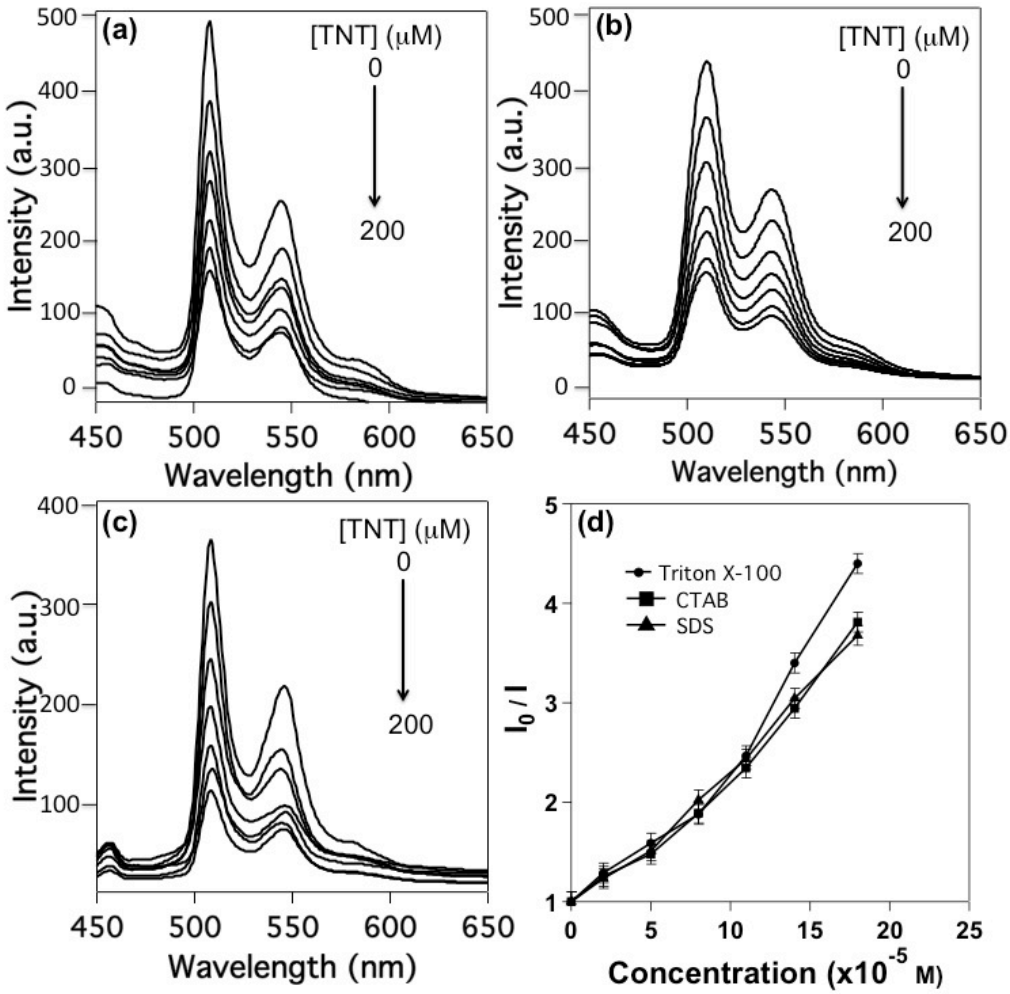

Figure S24: PL titration results of **2•Pt**/micelle adducts in water with incremental addition of TNT to (a) Triton X-100 micelle, (b) SDS micelle, (c) CTAB micelle; and (d) Stern-Volmer plots obtained from the above three titration results.

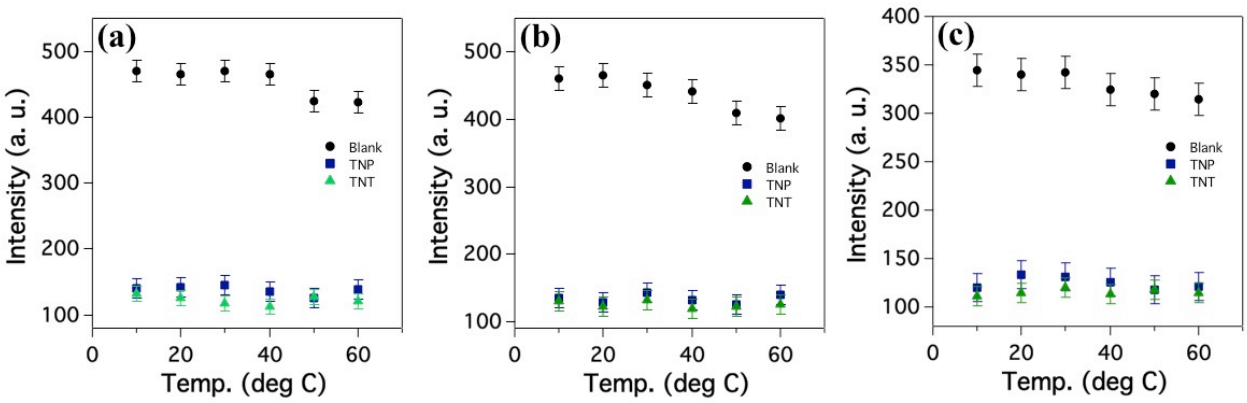

Figure S25: PL spectra of **2•Pt**/micelle adducts in water at variable temperature obtained with and without addition of 200 μM of TNT and TNP; (a) Triton X-100 micelle, (b) SDS micelle, (c) CTAB micelle.

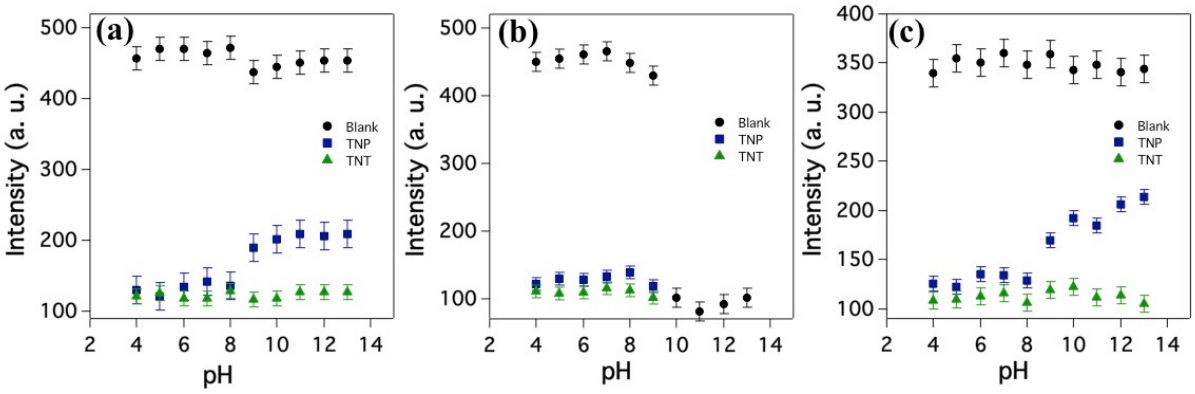

Figure S26: PL spectra of **2•Pt**/micellar adducts in water at variable pH ranges obtained with and without addition of 200 μM of TNT and TNP to (a) Triton X-100, (b) SDS, (c) CTAB respectively. Buffer solutions and their corresponding concentrations are as follows: for pH (4.0, 5.0), CH_3COOH–CH_3COONa (0.02 M); pH (6.0–8.0), NaH_2PO_4–Na_2HPO_4 (0.02 M); pH (9.0–11.0), $NaHCO_3$–Na_2CO_3 (0.02 M); pH 12.0, NaH_2PO_4–NaOH (0.02 M); and pH 13.0, KCl–NaOH (0.02 M). (Ref S2)

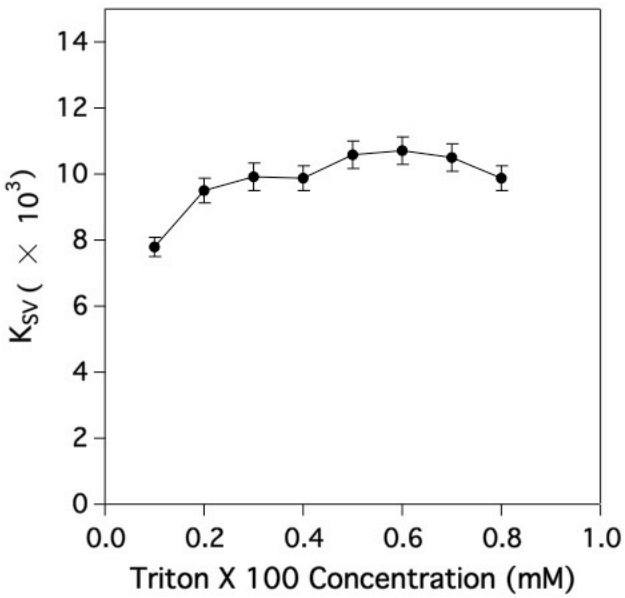

Figure S27: Stern-Volmer constants (K_{sv}) for TNP and **2•Pt**/Trition X-100 miceller interactions with varying concentration of Triton X-100.

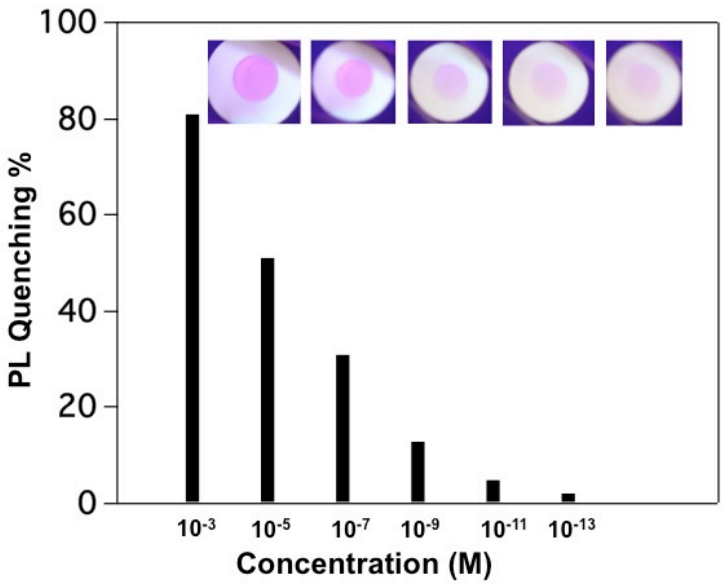

Figure S28: The quenching efficiency of **2•Pt** impregnated paper strip with addition of 20 μL of TNT solution with varying concentration.

D. References

S1. (a) Koo, C.-K.; Ho, Y.-M.; Chow, C.-F.; Lam, M. H.-W.; Lau, T.-C.; Wong, W.-Y. *Inorg. Chem.* **2007**, *46*, 3603–3612. (b) Koo, C.-K.; So, L. K.-Y.; Wong, K.-L.; Ho, Y.-M.; Lam, Y.-W.; Lam, M. H.-W.; Cheah, K.-W.; Cheng, C. C.-W.; Kwok, W.-M.; *Chem. Eur. J.* **2010**, *16*, 3942–3950. (c) Jana, A.; McKenzie, L.; Wragg, A, B.; Ishida, M.; Hill, J. P.; Weinstein, J. A.; Baggaley, E.; Ward, M. D. *Chem. Eur. J.*, **2016**, *22*, 4164–4174.

S2. Bai, M.; Huang, S.; Xu, S.; Hu, G.; Wang, L. *Anal.Chem*. **2015**, *87*, 2383–2388.